Ocean Sci. Discuss., 8, 397–433, 2011
www.ocean-sci-discuss.net/8/397/2011/
doi:10.5194/osd-8-397-2011

Ocean Science Discussions

Operative forecast of hydrophysical fields in the Georgian Black Sea coastal zone within the ECOOP

A. A. Kordzadze and D. I. Demetrashvili

M. Nodia Institute of Geophysics, Iv. Javakhishvili Tbilisi State University, 1, M. Alexidze Str., 0193 Tbilisi, Georgia

Received: 31 December 2010 – Accepted: 3 February 2011 – Published: 21 February 2011

Correspondence to: D. I. Demetrashvili (demetr_48@yahoo.com)

Published by Copernicus Publications on behalf of the European Geosciences Union.

Operative forecast of hydrophysical fields

A. A. Kordzadze and D. I. Demetrashvili

Abstract

One of the part of the Black Sea Nowcasting/Forecasting System is the regional forecasting system for the Easternmost part of the Black Sea (including the Georgian water area), which have been developed within the context of the EU International projects ARENA and ECOOP. A core of the regional system is a high-resolution baroclinic regional model of the Black Sea dynamics developed at M. Nodia Institute of Geophysics (RM-IG). This model is nested in the basin-scale model (BSM) of Marine Hydrophysical Institute (MHI, Sevastopol/Ukraine). The regional area is limited to the Caucasian and Turkish coastal lines and the western liquid boundary coinciding with a meridian 39.36° E. Since June 2010 we regularly compute 3 days' forecasts of current, temperature and salinity for the Easternmost part of the Black Sea with 1 km spacing. In this study results of two forecasts are presented. The first forecast corresponds to Summer season and covers the prognostic interval from 00:00 h, 6 August to 00:00 h, 9 August 2010. The second one corresponds to Autumn season and covers the prognostic interval from 00:00 h, 26 October to 00:00 h, 29 October 2010. Data needed for the forecasts – the 3-D initial and prognostic hydrophysical fields, also 2-D prognostic meteorological fields at the sea surface, wind stress, heat fluxes, evaporation and precipitation rates for the our regional area are placing on the MHI server every day and we are available to use these data operatively. Prognostic hydrophysical fields are results of forecast by BSM of MHI and 2-D meteorological boundary fields represent results of forecast by regional atmospheric model ALADIN. All these fields are given on the grid of BSM with 5 km spacing and with one-hour time step frequency for the integration period. The analysis of predicted fields shows that to use the model with high resolution is very important factor for identification of nearshore eddies of small sizes. It should be noted very different character of regional circulation in summer and autumn seasons in the Easternmost part of the Black Sea.

1 Introduction

Large scientific and technical achievement of the Black Sea operative oceanography for the last decade is development of the Black Sea Nowcasting/Forecasting System which allows to carry out continuous control over a current state of the Black Sea and its change for some days forward (Besiktepe, 2003; Korotaev and Eremeev, 2006). Creation of such system was promoted in a greater degree by the works performed by the leading oceanographic Centers of the Black Sea riparian countries within the EU International scientific and technical projects ARENA and ECOOP. Coordination of these works was carried out by Marine Hydrophysical Institute (MHI, Sevastopol, Ukraine) of the National Academy of Sciences of Ukraine. Functioning of the system in operative mode is especially important for coastal and shelf areas which undergoes the greatest anthropogenous loading.

The main structure of the Nowcasting/Forecasting System is described by Korotaev et al. (2006) and Kubryakov et al. (2006). One of the part of the System is the regional forecasting system for the Easternmost part of the Black Sea (including the Georgian water area), the core of which is a high-resolution baroclinic regional model (RM-IG) of the Black Sea dynamics developed at M. Nodia Institute of Geophysics by Kordzadze and Demetrashvili (2008, 2010). This model is nested in the basin-scale model (BSM) of the Black Sea dynamics of MHI (Demyshev and Korotaev, 1992). Note that the pilot real-time operation of the Black Sea Nowcasting/Forecasting System (including regional forecasting system for the Georgian water area) was successfully carried out for the first time in July 2005 during five days (Kubryakov et al., 2006; Kordzadze and Demetrashvili, 2008).

Since June 2010 at M. Nodia Institute of Geophysics 3 days' forecasts of 3-D fields of current, temperature and salinity with high resolution are regularly carried out for the Easternmost part of the Black Sea. All input data needed for initial and boundary conditions are available from the MHI server.

In this study we consider the regional forecasting system for the Easternmost part of the Black Sea and with the purpose of demonstrating the functioning of the system, two forecasts of hydrophysical fields for summer and autumn seasons, when circulating features of waters of the Georgian coastal zone significantly differed from each other, are discussed.

2 Regional forecasting system

The main component of the regional forecasting system the RM-IG is developed by adaptation of the BSM of the Black Sea dynamics of M. Nodia Institute of Geophysics (Kordzadze and Demetrashvili, 2004; Kordzadze et al., 2008; Demetrashvili et al., 2008) to the Easternmost part of the basin and nesting in the BSM of MHI. It is necessary to note that in turn the BSM of Institute of Geophysics is an improved version of the prognostic model of the Black Sea dynamics (Kordzadze and Skiba, 1973; Marchuk et al., 1975; 1979; Marchuk and Kordzadze, 1986; Kordzadze, 1989) originally developed in the early 1970s at the Computing Center of Siberian Branch of the Academy of Sciences USSR (Novosibirsk, Akademgorodok).

2.1 Model description

The RM-IG is based on a primitive system of ocean hydro-thermodynamics equations in hydrostatic approximation, which is written in z- coordinates for deviations of thermodynamic values from their standard vertical distributions (Kordzadze and Demetrashvili, 2008, 2010).

The model equation system is given in Appendix A. The model takes into account: nonstationary atmospheric wind and thermohaline forcing, quasi-realistic bottom relief, the absorption of solar radiation by the sea upper layer, space-temporal variability of horizontal and vertical turbulent exchange (Appendix B).

OSD

8, 397–433, 2011

Atmospheric forcing is taken into account by boundary conditions on the sea surface considered as a rigid surface, where Neumann conditions are used by given of wind stress components, heat fluxes, precipitation and evaporation from the sea surface. On the sea bottom the velocity components, heat and salt fluxes are equal to zero. On the lateral surfaces, two kinds of boundary conditions are considered: (a) on the rigid boundaries, sharing the sea from the land, components of current velocity, gradients of temperature and salinity normal to the boundary surface are equal to zero; (b) on the liquid boundary prognostic values of velocity, temperature and salinity computed on the base of BSM of MHI are used.

2.2 Method of solution

The existence and uniqueness theorems of 3-D nonstationary problem of the sea dynamics are proved by Sukhonosov (1981) and Kordzadze (1982). To solve the problem we used the two-cycle method of splitting the model equation system with respect to both physical processes and coordinate planes and lines, which was proposed to solve problems of ocean and atmosphere dynamics by Marchuk (1967, 1974).

Let's describe the numerical algorithm briefly. After splitting of the model equation system (see Appendix A) with respect to physical processes the following main stages are allocated: (1) The transfer of the physical fields taking into account eddy viscosity and diffusion; (2) The adaptation of the physical fields with division of the solution into barothropic and baroclinic components. For approximation on time of all split problems the Krank-Nickolson scheme is used.

At the transfer stage, after using two-cycle splitting method with respect to coordinates and corresponding transformation, we receive one-dimensional finite-difference equations on coordinates x, y, and z for grid functions of velocity components u and v, temperature deviations T and salinity deviations S. The received equations are solved by the factorization method.

OSD
8, 397–433, 2011

At the adaptation stage the barothropic and baroclinic components are allocated. The barothropic task is reduced to solution of 2-D finite-difference equation for integral stream function.

The differential operator of the baroclinic problem is preliminary split with the purpose of allocating the term describing the Coriolis force action as an independent stage. The remaining part of the differential operator of the baroclinic problem after using finite-difference approximation is split on vertical coordinate planes zx and zy. As a result, a set of 2-D problems for baroclinic components on vertical planes are received, which then also are reduced to the equations for analogs of stream functions.

Thus, the adaptation problem as a whole is reduced to solution of sequence of the same type 2-D problems for the stream function and analogs of stream functions, which are efficiently realized within the framework of uniform iterative algorithm (Kordzadze, 1989). The exception is a task considering the Coriolis force action, which is explicitly realized by solution of algebraic equations. At the transfer stage all required grid functions are defined in grid points with integer indexes, and at the stage of adaptation the functions are defined on the shifted grids. Transition from one grid to another is carried out by the linear interpolation.

The finite-difference schemes received at each elementary stage of splitting are absolutely steady, energetically balanced and provide the second order accuracy on time and space coordinates (in case of uniform grid). To use the splitting method substantially simplifies the implementation of complex physical model and enables us to reduce solution of 3-D nonstationary problem to solution of more simple 2-D and 1-D problems.

2.3 Methodology of nested grid modeling and some input parameters

The high-resolution RM-IG of the Black Sea dynamics (with grid step 1 km) is nested in the BSM of MHI (with grid step 5 km). The regional area is bounded with the Caucasus and Turkish shorelines and the western liquid boundary coincident with 39.36° E. The regional domain is covered with grid having on horizons 193 × 347 points. On a vertical the non-uniform grid with 30 calculated levels on depths: 2, 4, 6, 8, 12, 16, 26, 36, 56,

OSD
8, 397–433, 2011

86, 136, 206, 306, . . . , 2006 m are considered. The time step is equal to 0.5 h.

Data needed for the forecasts – the 3-D initial and prognostic hydrophysical fields, also 2-D prognostic meteorological fields at the sea surface – wind stress, heat fluxes, evaporation and precipitation rates for our regional area are placing on the MHI server every day and we are available to use these data operatively. Prognostic hydrophysical fields are results of forecast by BSM of MHI and 2-D meteorological boundary fields represent results of forecast by regional atmospheric model ALADIN. All these fields are given on the grid of BSM with one-hour time step frequency for the 4 days period. With the purpose of using the received data as initial and boundary conditions (on upper and liquid boundaries) for RM-IG, during model implementation these fields are transferring to grid of RM-IG with 1 km spacing by interpolation.

Concerning the input data it is necessary to note the following. The input data, which are given on a course grid, provide to run for 4 days, but we consider that the RM-IG gives forecast only for three days as during the first day the coastal model runs in the prognostic mode only to have better adjustment of the fine resolution to the coarse initial conditions provided by the BSM of MHI.

The software of the problem is developed on the basis of the algorithmic language "Compaq Visual Fortran 6.1", and realization of the forecasting system is carried out on PC Pentium-4 with 3.00 GHz. The system allows to calculate 3-D fields of current, temperature, salinity and density in the Black Sea coastal zone with 1 km resolution. At 24, 48, and 72 h after starting the forecast visualization of the flow, temperature and salinity fields on horizons 0, 10, 20, 50, 100, 200, 500, 1000 m is carried out using the System software "Surfer –8". Transition from calculated levels to these ones is carried out by the linear interpolation.

3 Simulation and forecast of regional circulation processes

To demonstrate the operation of the regional forecasting system, there are considered two examples of the forecast corresponding to Summer and Autumn seasons, when

OSD
8, 397–433, 2011

circulating features of waters of the Georgian Black Sea coastal zone area extremely differed from each other.

3.1 Forecast for summer season

The forecasting time period was from 00:00 h, 6 August to 00:00 h, 9 August 2010 (here and after local time is used), but according to discussed above, integration of model equations began one day earlier, i.e. at 00:00 h, 5 August. At this moment the current field in the regional area on the different depths is shown in Fig. 1. From this Figure it is clear that the main element of the regional circulation is the anticyclonic eddy (called the Batumi eddy) with diameter about of 150–200 km, which covers the significant part of the considered area. This vortex practically does not change in the upper 200 m layer, only current speed decreases from maximal value equal to 24 cm/s till 11 cm/s, below 200 m the vortex gradually decreases in sizes (Fig. 1d). At deeper levels the Batumi eddy gradually disappeared.

The temperature and salinity fields on the Black Sea surface and horizon $z = 100$ m at the beginning of integration of model equation system are presented in Figs. 2 and 3. Horizontal distribution of the surface temperature is typical for the summer period, warmer waters are in the Caucasus nearshore zone. On the horizon $z = 100$ m the cold intermediate layer (CIL), which covers a considerable part of the allocated water area is well observed (CIL is bounded with isotherm of 8 °C). The Batumi anticyclonic eddy makes appreciable impact on formation of salinity field in the considered area. General feature of this field is that the area of relatively low salinity waters coincides with allocation of anticyclonic eddy (compare Figs. 1 and 3). It is easy to explain this fact to that descending streams, which develop in the anticyclonic vortex, transfer less salty waters from the upper layer downwards (Stanev et al., 1988; Kordzadze, 1989).

The analysis of the wind stress fields for the forecasting period showed that atmospheric circulation significantly changed during this period (Fig. 4).

The surface current fields after 24, 48, and 72 h (time is counted from the initial moment of the forecast, 00:00 h, 6 August 2010), predicted by the RM-IG, are presented

OSD
8, 397–433, 2011

in Fig. 5 and the same fields predicted by the BSM of MHI at the same time moments are shown in Fig. 6. The comparative analysis of Figs. 5 and 6 shows that the results of forecast of the Batumi eddy predicted by both models are practically the same. Accordance to both models this eddy is rather stable formation and it is observed during all forecasting period without strong changes, despite nonstationarity of atmospheric forcing. It must be noted that formation of the anticyclonic eddy in the south-east part of the Black Sea basin and its stability in Summer season is a well-known fact (Oguz et al., 1993; Korotaev et al., 2003).

Sea circulation patterns predicted by both RM-IG and BSM of MHI considerably differ from each other in the narrow zone with width about 20–25 km along the Caucasian shoreline. The system of currents in this zone by results of RM-IG is characterized by the clear tendency to vortex formation of very small sizes and nonstationarity, whereas results of BSM specify about smoothness and practically non-stationary character of current in this zone. For example, unlike results of the BSM, in Fig. 5a formation of a small cyclonic eddy with a diameter about 15–20 km near the Sukhumi water area is well visible at $t = 24$ h, which further undergoes some modification in time. The existence of rather unstable eddies of small sizes of cyclonic and anticyclonic characters near the Georgian shoreline is known from observations (Jaoshvili, 1986), but their identification by the mathematical models is possible by providing very high resolution, that is achieved in the RM-IG.

Temperature and Salinity fields predicted by the RM-IG are presented in Figs. 7 and 8, and the same fields predicted by the BSM of MHI – in Figs. 9 and 10. In both cases these fields are shown on depth of 10 m and at moments 24 and 72 h after start of the forecast. Comparison between Figs. 7 and 9 shows some differences of temperature patterns computed on the basis RM-IG and BSM of MHI. From these Figures is visible that in both cases colder waters are observed in the central area of the Batumi eddy than on its peripheries, but this feature is more expressed in the temperature field predicted by the BSM (Fig. 9). Comparison of Figs. 8 and 10 obviously demonstrate efficiency of the higher resolution model to simulate a salinity field in the coastal zone

OSD
8, 397–433, 2011

A. A. Kordzadze and D. I. Demetrashvili

with higher adequacy. From Fig. 8 it is well visible the zone with high salinity, having a form of concave tongue, that apparently shows transfer of more salty waters from the open part of the sea into the Georgian water area by the Batumi eddy. The coarse resolution model is unable to reproduce this phenomenon (Fig. 10), whereas the fine intrusion of waters of different salinity is well resolved by the high resolution RM-IG.

It should be noted that only comparison of modeling results to the natural data corresponding to the considered period can definitely answer the question what results from these models are close to the real data. Unfortunately, we couldn't make such comparisons yet because of complexity to find corresponding measurements of temperature and salinity in the considered area.

3.2 Forecast for Autumn season

The second example of the forecast concerns to the Autumn, when the forecasting period was from 00:00 h, 26 October to 00:00 h, 29 October 2010. Like the previous case, integration of model equation system began one day earlier, at 00:00 h, 25 October.

The velocity pattern on some horizons at the beginning of integration is shown in Fig. 11. It is interesting to note that the character of the regional circulation is quite different from circulation taking place on 5 August 2010 (see Fig. 1). The general structure of the regional circulation on 00:00 h, 25 October is characterized by formation of cyclonic and anticyclonic eddies of small sizes. Such structure is qualitatively kept up to deep levels with gradual reduction of the maximal speed of the flow from 32 cm /s up to 4 cm/s on horizon z = 500 m. Accordingly, horizontal distributions of temperature and salinity fields (Figs. 12 and 13) differ from distribution of the same fields at 00:00, 5 August 2010 (see Figs. 3 and 4)

The Atmospheric wind above the regional area considerably changed during the forecasting interval (Fig. 14).

The prognostic surface regional circulation patterns computed by the RM-IG are presented in Fig. 15 and the same patterns computed by the BSM of MHI are demonstrated in Fig. 16 at moments 24, 48, and 72 h after start of the forecasting interval.

Comparison of these two figures directs us to the idea, that high resolution of numerical model is a major factor for improving identification of small unstable eddies which are permanently formed in the coastal zone.

The prognostic fields of temperature and salinity computed by the RM-IG are shown in Figs. 17 and 18 and the same fields predicted by the BSM are presented in Fig. 19 and 20. These fields are shown on the depth of 10 m after 48 and 72 h after the initial moment of the forecast. The comparative analysis of the fields predicted by both RM-IG and BSM shows, that in this case temperature and salinity fields predicted by both models are qualitatively and quantitatively close to each other.

4 Conclusions

A regional forecasting system allowed to predict flow, temperature and salinity fields with 1 km spacing in the Easternmost part of the Black Sea (including Georgian water area) is elaborated. The core of the forecasting system is the hydrostatic baroclinic regional model of the Black Sea dynamics developed at M. Nodia Institute of Geophysics, which is nested in the BSM of MHI.

The simulation and 3 days' forecasts of 3-D hydrophysical fields were performed for the Summer and Autumn seasons 2010 using the prognostic data of BSM of MHI and atmospheric dynamics model ALADIN.

The model simulation shows the seasonal differences between regional dynamical processes. Our results once again show already known fact that in the summer the main element of the regional circulation in the considered area is the Batumi anticyclonic eddy. Unlike the summer circulation, in the autumn the circulation has a vortical character with formation of cyclonic and anticyclonic eddies with diameters about 20–40 km. These eddies are not stable formations and decompose or undergoes some modifications in time.

The comparative analysis of predicted fields by both RM-IG and BSM of MHI shows that to use the model with high resolution is very important factor for identification of

OSD
8, 397–433, 2011

coastal eddies of small sizes. In case of forecast of summer circulation more differences are observed in the narrow zone along Caucasus shoreline. In this near-shore zone the flow predicted by the RM-IG is characterized by nonstationarity and the tendency to form eddies of small sizes. Such character of the sea flow along the Georgian near-shore zone is known from observations (Jaoshvili, 1986). In case of forecast of autumn circulation considerable differences between the predicted current fields are observed: the vortex formation processes are more intensive at using of the RM-IG. It is also interesting fact that in summer, when the Batumi eddy is well developed, penetration of more salty waters from the open part of the Black Sea into the Georgian water area is distinctly observed by the results of the RM-IG.

Finally, it must be noted that unfortunately we did not have an opportunity to compare predicted fields with real data because it was not easy to find real data corresponding to the considered regional area. However, such comparisons have been done during the pilot experiment within the project ARENA in 2005, which showed an ability of the RM-IG to predict hydrophysical fields with sufficient accuracy (Kubryakov et al., 2006).

Appendix A

Model equation system

The RM-IG equation system, which describes the hydro and thermodynamic processes in the sea basin, is following:

$$\frac{\partial u}{\partial t}+\mathrm{div}\boldsymbol{u}u-lv+\frac{1}{\rho_0}\frac{\partial p'}{\partial x}=\nabla\mu\nabla u+\frac{\partial}{\partial z}\nu\frac{\partial u}{\partial z},$$

$$\frac{\partial v}{\partial t}+\mathrm{div}\boldsymbol{u}v+lu+\frac{1}{\rho_0}\frac{\partial p'}{\partial y}=\nabla\mu\nabla v+\frac{\partial}{\partial z}\nu\frac{\partial v}{\partial z},$$

$$\frac{\partial p'}{\partial z}=g\rho', \quad \mathrm{div}\boldsymbol{u}=0,$$

OSD
8, 397–433, 2011
Operative forecast of hydrophysical fields
A. A. Kordzadze and D. I. Demetrashvili

$$\frac{\partial T'}{\partial t}+\mathrm{div}\boldsymbol{u}T'+\gamma_T.w=\nabla\mu_T\nabla T'+\frac{\partial}{\partial z}\nu_T\frac{\partial T'}{\partial z}+\frac{\partial \nu_T\gamma_T}{\partial z}-\frac{1}{c\rho_0}\frac{\partial I}{\partial z}-\frac{\partial \bar{T}}{\partial t},$$

$$\frac{\partial S'}{\partial t}+\mathrm{div}\boldsymbol{u}S'+\gamma_S w=\nabla\mu_S\nabla S'+\frac{\partial}{\partial z}\nu_S\frac{\partial S'}{\partial z}+\frac{\partial \nu_S\gamma_S}{\partial z}-\frac{\partial \bar{S}}{\partial t},$$

$$\rho'=\alpha_T T'+\alpha_S S',\quad \gamma_T=\frac{\partial \bar{T}}{\partial z},\gamma_S=\frac{\partial \bar{S}}{\partial z},$$

$$T=\bar{T}(z,t)+T',S=\bar{S}(z,t)+S',\rho=\bar{\rho}(z,t)+\rho',p=\bar{p}(z,t)+p',$$

$$\nabla\mu\nabla=\frac{\partial}{\partial x}\mu\frac{\partial}{\partial x}+\frac{\partial}{\partial y}\mu\frac{\partial}{\partial y},\quad I=\eta(1-A)I_0e^{-\alpha z},$$

$$I_0=a\ \mathrm{sinh}_0-b\sqrt{\mathrm{sinh}_0},\quad \mathrm{sinh}_0=\ \sin\varphi\sin\psi+\cos\varphi\cos\psi\cos\frac{\pi}{12}t,\quad \eta=1-(\tilde{a}+\tilde{b}\tilde{n})\tilde{n}.$$

$$\alpha_T=\partial f/\partial\bar{T}=-10^{-3}(0.0035+0.00938\bar{T}+0.0025\bar{S}),$$

$$\alpha_S=\partial f/\partial s=10^{-3}.(0.802-0.002\bar{T}).$$

Here are used the following notations: u, v, and w are the components of the current velocity vector along the axes x, y, and z, respectively (the axes x, y, and z are directed eastward, northward, and vertically downward from the sea surface, respectively); T',S',P',ρ' are the deviations of temperature, salinity, pressure and density from their standard vertical distributions $\bar{T},\bar{S},\bar{P},\bar{\rho}$; $l=l_0+\beta.y$ is the Coriolis parameter, where $\beta=dl/dy$; g, c, and ρ_0 are the gravitational acceleration, the specific heat capacity and average density of seawater, respectively; $\mu,\mu_{T,S},\nu,\nu_{T,S}$ are the horizontal and vertical eddy viscosity, heat and salt diffusion coefficients, respectively; I_0- the total flux of solar radiation at $z=0$; A is the albedo of a sea surface, h_0 is the zenithal angle of the Sun; φ is the geographical latitude,Ψ is the parameter of declination of the Sun, η is the factor which takes into account influence of a cloudiness on a total radiation and depends upon ball of cloudiness $\tilde{n}$ (Berlyand, 1960); a, b, $\tilde{a}$, $\tilde{b}$ are the empirical factors; $\alpha$is the parameter of absorption of short-wave radiation by seawater.

OSD
8, 397–433, 2011

Title Page
Abstract | Introduction
Conclusions | References
Tables | Figures
◂◂ | ▸▸
◂ | ▸
Back | Close
Full Screen / Esc
Printer-friendly Version
Interactive Discussion

Appendix B

Parameterization of the turbulent field

Factors of horizontal viscosity and diffusion for temperature and salt μ, $\mu_{T,S}$ where calculated by the formulas (Zilitinkevich and Monin, 1971)

$$\mu = \Delta x . \Delta y \sqrt{2\left(\frac{\partial u}{\partial x}\right)^2 + \left(\frac{\partial u}{\partial y} + \frac{\partial v}{\partial x}\right)^2 + 2\left(\frac{\partial v}{\partial y}\right)^2}, \quad \mu_T = \frac{\mu}{c_T}, \quad \mu_S = \frac{\mu_S}{c_S},$$

where Δx and Δy are horizontal grid steps along x and y respectively, c_T and c_S are some constants equal to 10.

Factors of vertical turbulent diffusion for heat and salt $\nu_{T,S}$ were calculated by using the modified Obukhov formula presented by Marchuk et al. (1980) as:

$$\nu_{T,S} = (0.05h)^2 \sqrt{\left(\frac{\partial u}{\partial z}\right)^2 + \left(\frac{\partial v}{\partial z}\right)^2 - \frac{g}{\rho_0}\frac{\partial \rho}{\partial z}}.$$

Here h is the depth of the turbulent surface layer, which is defined by the first point z_m, in which following condition is satisfied:

$$(0.05z_\mathrm{m})^2 \sqrt{\left(\frac{\partial u}{\partial z}\right)^2 + \left(\frac{\partial v}{\partial z}\right)^2 - \frac{g}{\rho_0}\frac{\partial \rho}{\partial z}} \leq \nu^0_{T,S}, \quad \nu^0_{T,S} = 1\mathrm{cm}^2\mathrm{s}^{-1}$$

Vertical turbulent viscosity factor

$$\nu = \begin{cases} 50\ \mathrm{cm}^2/s, & z \leq 55\ \mathrm{m} \\ 10\ \mathrm{cm}^2/s, & z > 55\ \mathrm{m} \end{cases}$$

In case of unstable stratification, which might appear during integration of the equations ($\frac{\partial \rho}{\partial z} < 0$), the realization of this instability in the model is taken into account by increase of factor of turbulent diffusion $\nu_{T,S}$ 20 times in appropriate columns from surface to a bottom.

Discussion Paper | Discussion Paper | Discussion Paper | Discussion Paper

OSD

8, 397–433, 2011

Acknowledgements. The Authors would like to thank the EU projects ARENA and ECOOP coordinators, G. Korotaev, O. Krarup Leth, P. Oddo, A. Kubryakov, also all other colleagues, with which the authors fruitfully cooperated within the implementation of these projects.

References

Berlyand, G. G.: Method of climatological calculation of the net radiation (in Russian), Meteorologia i gidrologia, Moscow, 6, 9–12, 1960.

Besiktepe, S. T.: Development of the regional forecasting system for the Black Sea, Proceeding of the "Second International Conference on Oceanography of Eastern Mediterranean and Black Sea: Similarities and Differences of Two Interconnected Basins", Ankara, Turkey, 14–18 October, 2002, 297–306, 2003.

Demetrashvili, D. I., Kvaratskhelia, D. U., and Gvelesiani, A. I.: On the vortical motions in the Black Sea obtained by the 3-D hydrothermodynamical numerical model, Adv. Geosci., 14, 295–299, doi:10.5194/adgeo-14-295-2008, 2008.

Demyshev, S. G. and Korotaev, G. K.: Numerical energy-balanced model of baroclinic currents in the ocean with bottom topography on the C-grid (in Russian), in: Numerical Models and Results of Intercalibration Simulations in the Atlantic Ocean, Moscow, 163–231, 1992.

Jaoshvili, Sh. V.: The river alluvium and the beach formation of the Georgian Black Sea coast (in Russian), Tbilisi, 155 pp., 1986.

Kordzadze, A. A.: Mathematical Problems of Solving Problems of Ocean Dynamics (in Russian), VTs SO AN SSSR, Novosibirsk, 148 pp., 1982.

Kordzadze, A. A.: Mathematical modelling of sea currents (theory, algorithms, numerical experiments) (in Russian), Moscow, OVM AN SSSR, 218 pp., 1989.

Kordzadze, A. A. and Demetrashvili, D. I.: Numerical modeling of inner-annual variability of the hydrological regime of the Black Sea with taking into account of alternation of different types of the wind above its surface, Proceed. of Intern. Conference: "A year after Johanesburg-Ocean Governance and Sustainable Development: Ocean and Coasts – a Glimpse into the Future", Kiev, Ukraine, 27–30 October 2003, 495–505, 2004.

Kordzadze, A. and Demetrashvili, D.: Simulation and forecast of hydrophysical fields in the part of the Georgian Black Sea coastal zone, J. Georgian Geoph. Soc., 12b, 7–16, 2008.

Kordzadze, A. and Demetrashvili, D.: Modeling of dynamical processes in the Black Sea,

Georgian Elecreonic Scientific Journal (GESJ): Physics, http://gesj.internet-academy.org.ge/phys/, 1(3) , 25–45, 2010.
Kordzadze, A. A. and Skiba, Yu. N.: Numerical calculations of the Black Sea with a three-dimensional model (in Russian), Preprint, Computer Center, Siberian Branch of Russian Academy of Sciences, Novosibirsk, 32 pp., 1973.
Kordzadze, A. A., Demetrashvili, D. I., and Surmava, A. A.: Numerical modeling of hydrophysical fields of the Black Sea under the conditions of alternation of atmospheric circulation processes, Izvestiya RAS, Atmospheric and Oceanic Physics, 44(2), 213–224, 2008.
Korotaev, G. K. and Eremeev, V. N.: Introduction in operative oceanography of the Black Sea, Sevastopol (in Russian), HPC "EKOCI-Gideofizika", 382 pp., 2006.
Korotaev, G., Oguz, T., Nikiforov, A., and Koblinsky, C.: Seasonal, interannual, and mesoscale variability of the Black Sea upper layer circulation derived from altimeter data, J. Geophys. Res., 108(C4), 3122, doi:10.1029/2002JC001508, 2003.
Korotaev, G., Cordoneanu, E., Dorofeev, V., Fomin, V., Grigoriev, A., Kordzadze, A., Kubriakov, A., Oguz, T., Ratner, Yu., Trukhchev, D., Slabakov, H.: Near-operational Black Sea nowcasting/forecasting system, in: European Operational Oceanography: Present and Future, 4th EuroGOOS Conference, 6–9 June 2005, Brest, France, 269–275, 2006.
Kubryakov, A., Grigoriev, A., Kordzadze, A., Korotaev, G., Trukhchev, D., Fomin, V.: Nowcasting/Forecasting subsystem of the circulation in the Black Sea nearshore regions, in: European Operational Oceanography: Present and Future. 4th EuroGOOS Conference, 6–9 June 2005, Brest, France, 605–610, 2006.
Marchuk, G. I.: Numerical methods in weather prediction (in Russian), Leningrad Gidrometeoizdat, 353 pp., 1967.
Marchuk, G. I.: Numerical Solution of Problems of Atmospheric and Oceanic Dynamics (in Russian), Gidrometeoizdat , Leningrad, 303 pp., 1974.
Marchuk, G. I. and Kordzadze, A. A.: Perturbation theory and the formulation of inverse problems of ocean dynamics (in Russian), Proceedengs of Tbelese State University, Mathematica, Mekhanica, Astronomia, 259(19–20), 49–65, 1986.
Marchuk, G. I., Kordzadze, A. A., and Skiba, Yu. N.: Calculation of major hydrological fields of the Black Sea on the basis of the splitting method., Izvestiya USSR, Atmos. Ocean. Phys., 11, 379–393, 1975.
Marchuk, G. I., Kordzadze, A. A., and Zalesnyi, V. B.: Problem of mathematical modelling of sea and ocean currents(in Russian), in: Differential and Integral Equations: Boundary-Value

OSD
8, 397–433, 2011

Problems, Tbilisi, 99–151, 1979.
Marchuk, G. I., Kochergin, V. P., Sarkisyan, A. S., Bubnov M. A., Zalesny, V. B., Klimok, V. I., Kordzadze, A. A., Kuznetsov, V. I., Protasov, A. B., Sukhorukov, B. A., Tsvetova, E. A., and Scherbakov, A. B.: Mathematical models of ocean circulation (in Russian), Nauka, Novosibirsk, 288 pp., 1980.
Oguz, T., Latun, V. S., Latif, M. A., Vladimirov, V. V., Sur, H. I., Markov, A. A., Ozsoy, E., Kotovshchikov, B. B., Eremeev, V. V., and Unluata, U.: Circulation in the surface and intermediate layers in the Black Sea, Deep. Sea Res. I, 40, 1597–1612, 1993.
Stanev E., Truhchev, D., and Roussenov, V.: The Black Sea circulation and its numerical modelling (in Russian), Sofia, Kliment Ohridski, 222 pp., 1988.
Sukhonosov, V. I.: On the correctness as a whole of a 3D problem of ocean dynamics, in: Mechanics of Inhomogeneous Continuous media (in Russian), Computer Center, Siberian Branch of Russian Academy of Sciences, Novosibirsk, 52, 37–53, 1981.
Zilitinkevich, S. S. and Monin, A. S.: Turbulence in Dynamic Models of the Atmosphere (in Russian), Nauka, Leningrad, 41 pp., 1971.

OSD
8, 397–433, 2011

A. A. Kordzadze and D. I. Demetrashvili

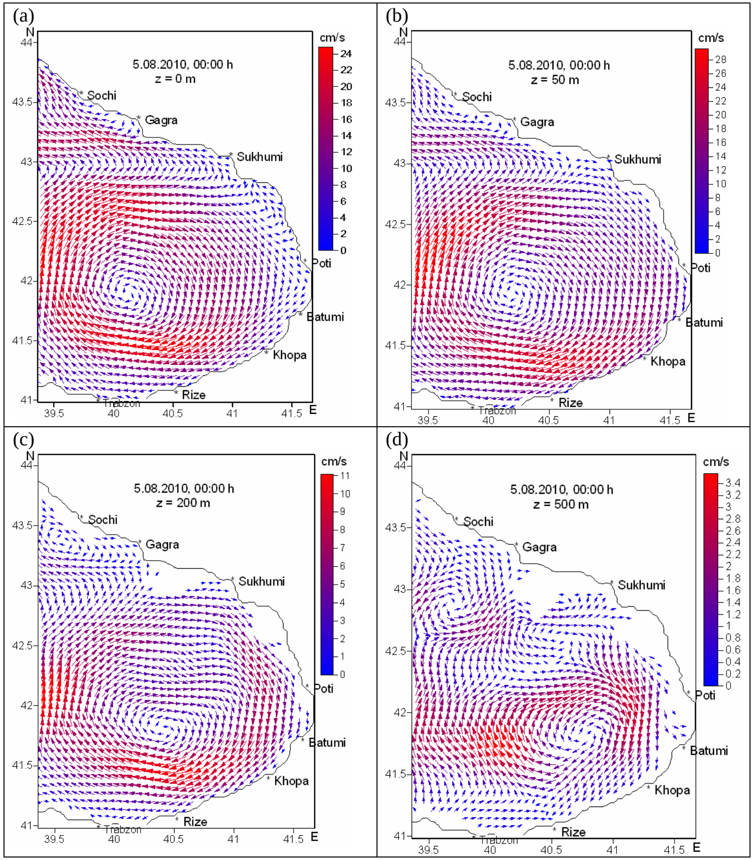

Fig. 1. Current field at 5 August 2010, 00:00 h on depths of 0 m **(a)**, 50 m **(b)**, 200 m **(c)**, and 500 m **(d)**.

OSD
8, 397–433, 2011

A. A. Kordzadze and D. I. Demetrashvili

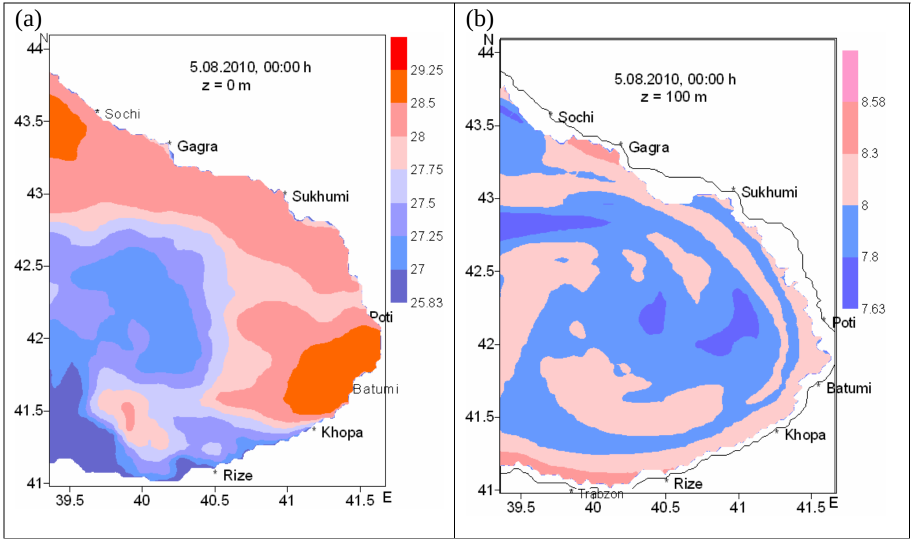

Fig. 2. Temperature field (deg. C) at 5 August 2010, 00:00 h on depths of 0 m **(a)** and 100 m **(b)**.

OSD
8, 397–433, 2011

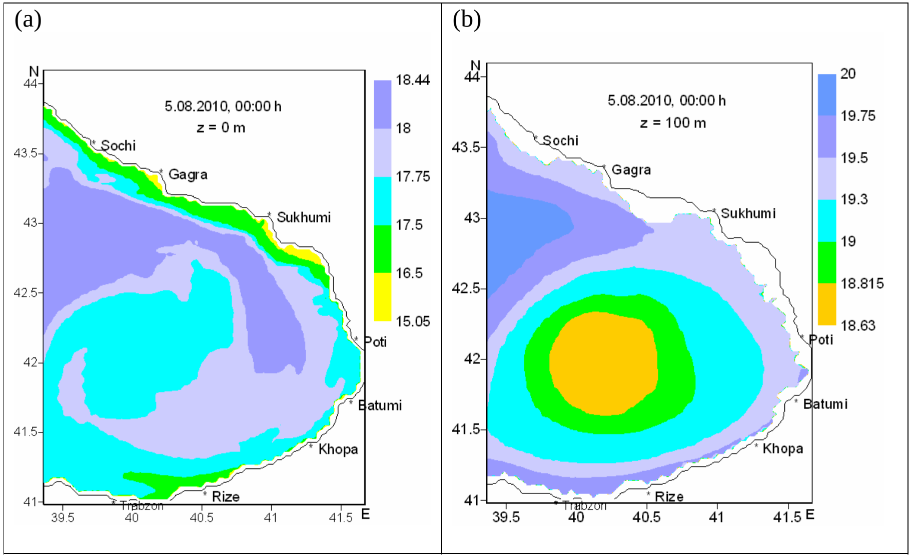

Fig. 3. Salinity field (psu) at 5 August 2010, 00:00 h on depths of 0 m **(a)** and 100 m **(b)**.

OSD
8, 397–433, 2011

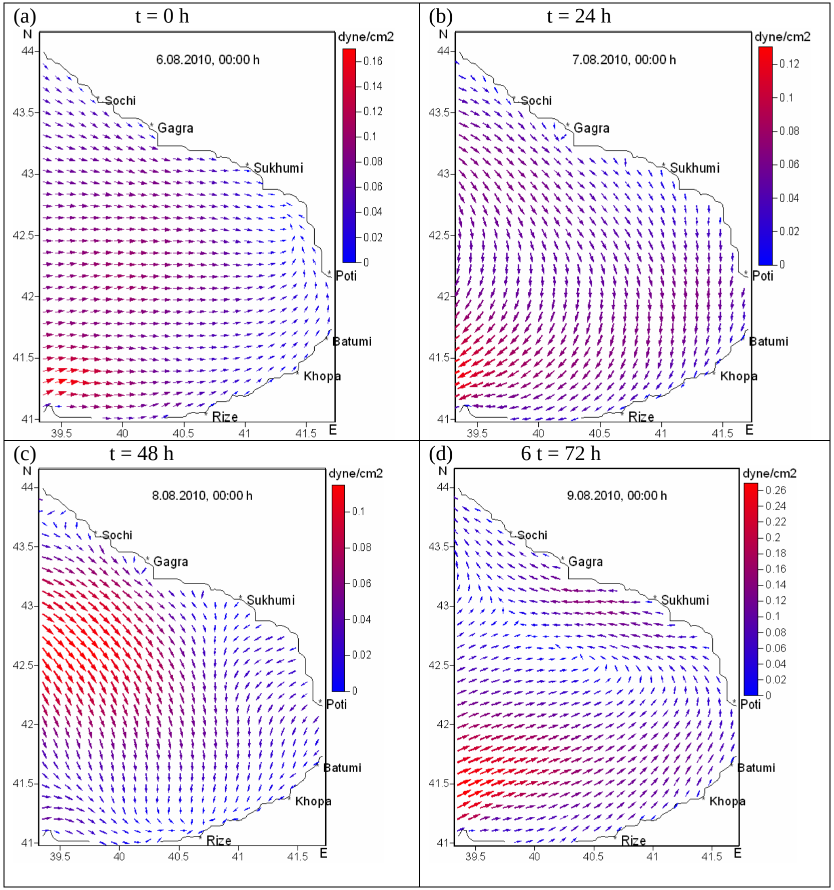

Fig. 4. Vector fields of the wind stress on the sea surface within the forecasting period: 6 August 2010, 00:00 h – 9 August 2010, 00:00 h at 0 h **(a)**, 24 h **(b)**, 48 h **(c)**, and 72 h **(d)** (here and in the following figures time is counted from the initial moment of the forecast).

OSD
8, 397–433, 2011

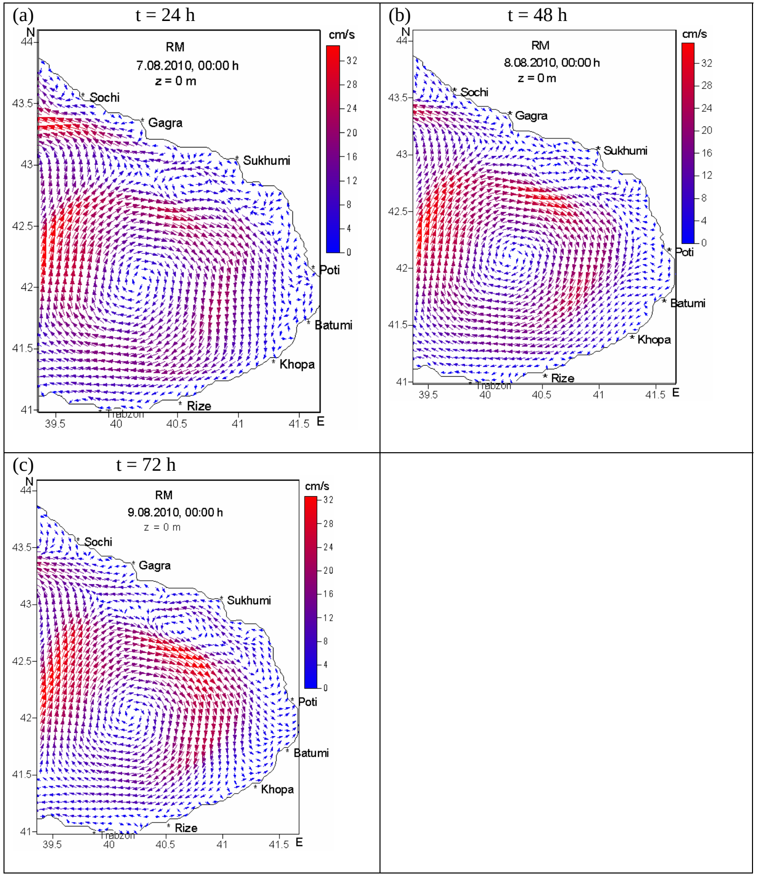

Fig. 5. The surface current fields predicted by RM-IG at 24 h **(a)**, 48 h **(b)**, and 72 h **(c)** (the forecasting period is 6 August 2010, 00:00 h – 9 August 2010, 00:00 h).

OSD
8, 397–433, 2011

A. A. Kordzadze and
D. I. Demetrashvili

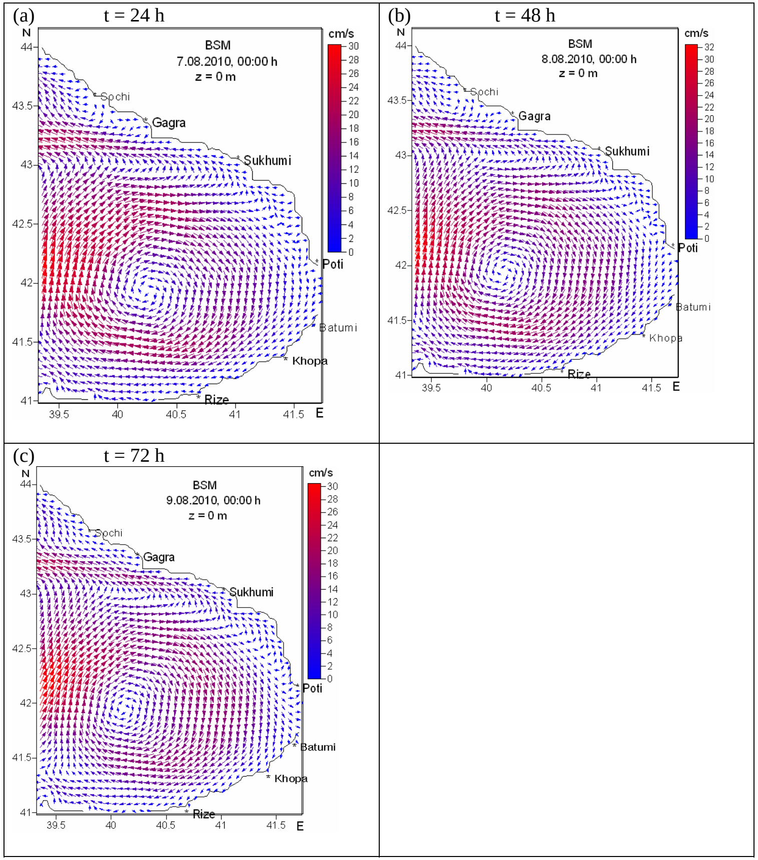

Fig. 6. The surface current fields predicted by BSM of MHI at 24 h **(a)**, 48 h **(b)**, and 72 h **(c)** (the forecasting period is 6 August 2010, 00:00 h – 9 August 2010, 00:00 h).

OSD
8, 397–433, 2011

Operative forecast of hydrophysical fields

A. A. Kordzadze and D. I. Demetrashvili

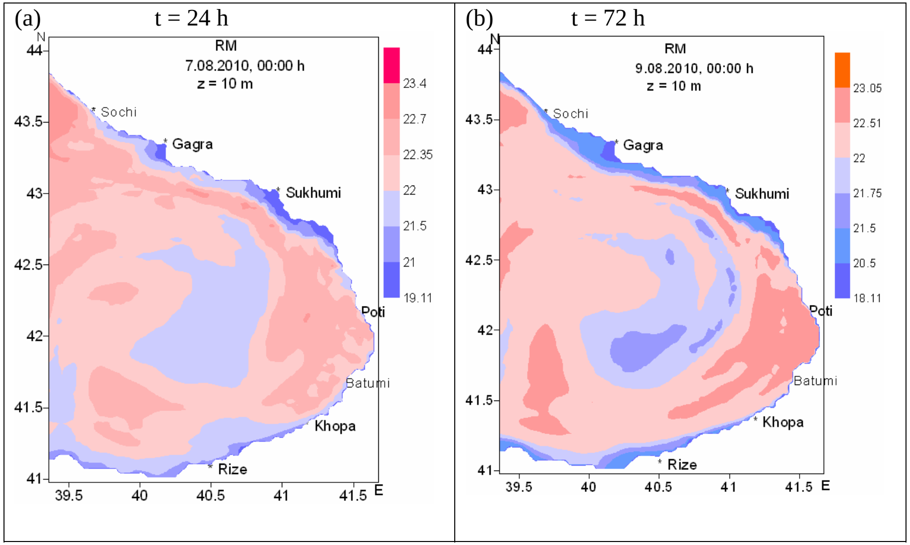

Fig. 7. The temperature fields (deg. C) on depth of 10 m predicted by RM-IG at **(a)** 24 h and **(b)** 72 h (the forecasting period is 6 August 2010, 00:00 h – 9 August 2010, 00:00 h).

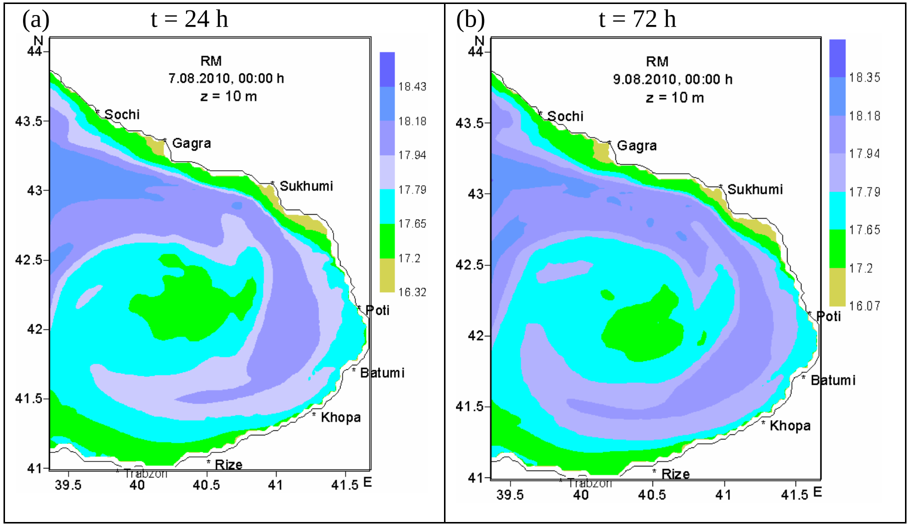

Fig. 8. The salinity fields (psu) on depth of 10 m predicted by RM-IG at **(a)** 24 h and **(b)** 72 h (the forecasting period is 6 August 2010, 00:00 h – 9 August 2010, 00:00 h).

OSD
8, 397–433, 2011

A. A. Kordzadze and D. I. Demetrashvili

Title Page
Abstract | Introduction
Conclusions | References
Tables | Figures
◀| |▶
◀ ▶
Back | Close
Full Screen / Esc
Printer-friendly Version
Interactive Discussion

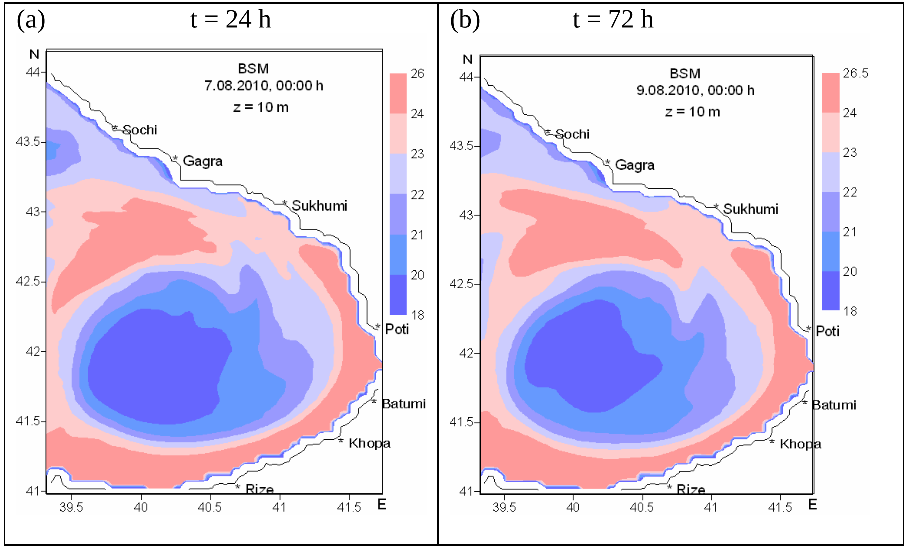

Fig. 9. The temperature fields (deg. C) on depth of 10 m predicted by BSM of MHI at **(a)** 24 h and **(b)** 72 h (the forecasting period is 6 August 2010, 00:00 h – 9 August 2010, 00:00 h).

OSD
8, 397–433, 2011

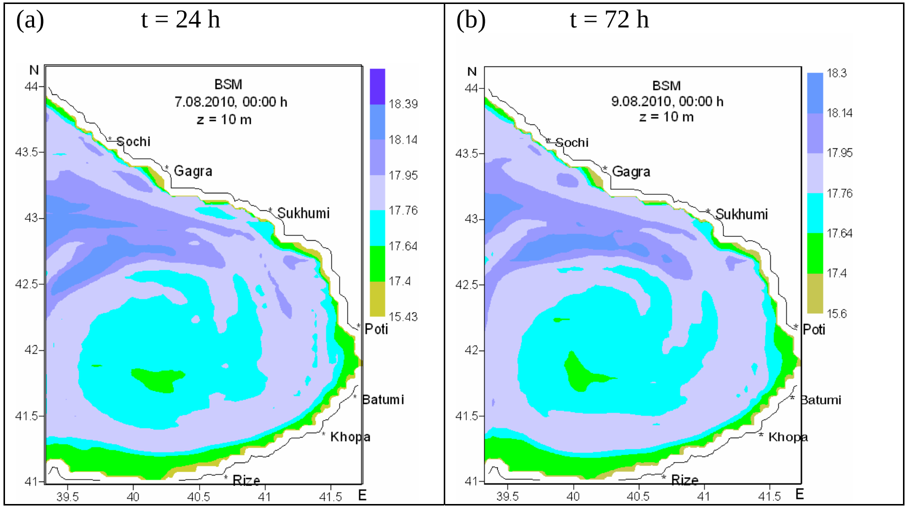

Fig. 10. The salinity fields (psu) on depth of 10 m predicted by BSM of MHI at **(a)** 24 h and **(b)** 72 h (the forecasting period is 6 August 2010, 00:00 h – 9 August 2010, 00:00 h).

OSD
8, 397–433, 2011

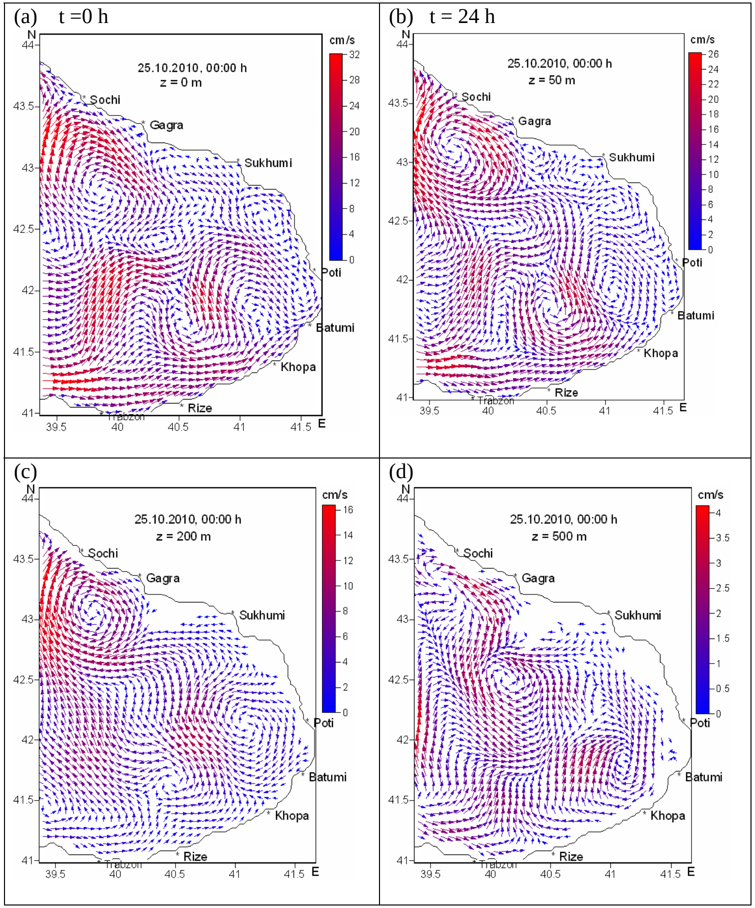

Fig. 11. Current field at 25 October 2010, 00:00 h on depths of **(a)** 0 m, **(b)** 50 m, **(c)** 200 m, and **(d)** 500 m.

OSD
8, 397–433, 2011

Operative forecast of hydrophysical fields

A. A. Kordzadze and D. I. Demetrashvili

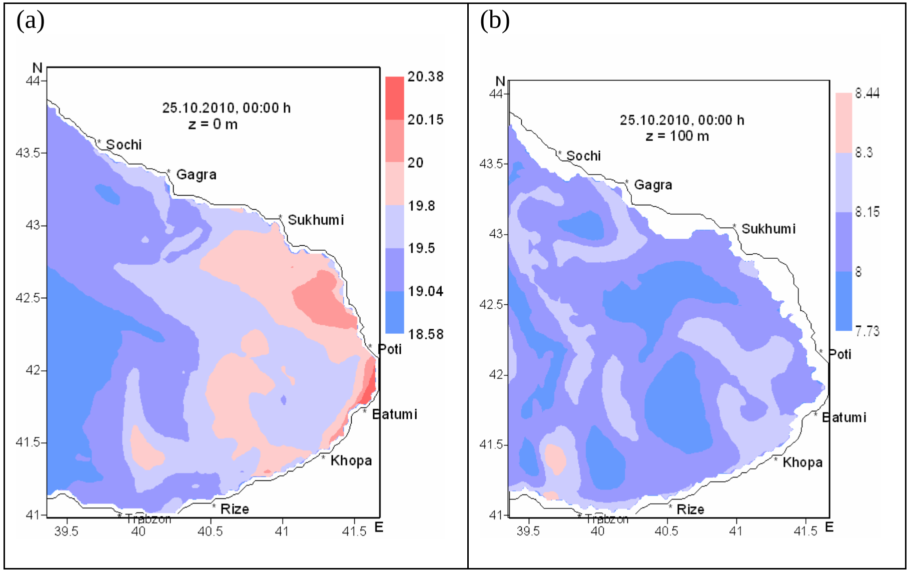

Fig. 12. Temperature field (deg. C) at 25 October 2010, 00:00 h on depths of **(a)** 0 m and **(b)** 100 m.

OSD
8, 397–433, 2011

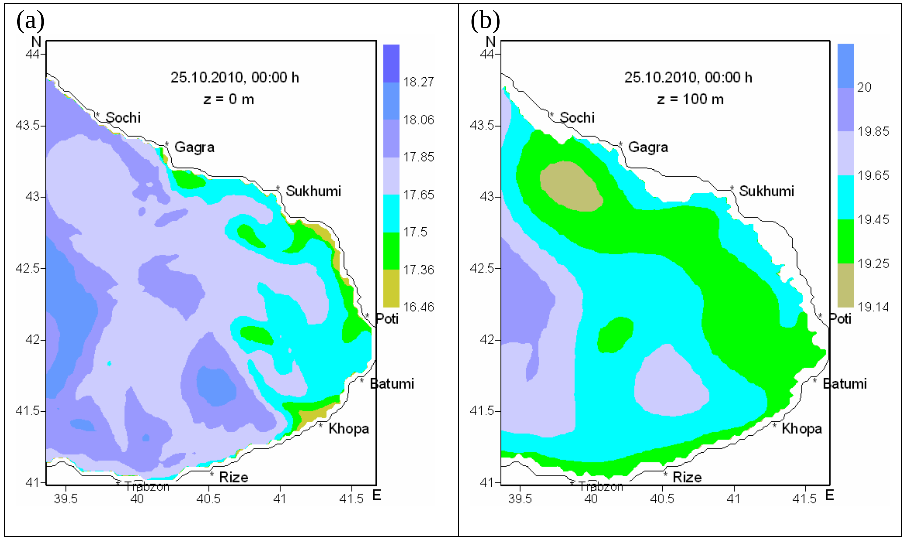

Fig. 13. Salinity field (psu) at 25 October 2010, 00:00 h on depths of **(a)** 0 m and **(b)** 100 m.

OSD
8, 397–433, 2011

Operative forecast of hydrophysical fields

A. A. Kordzadze and D. I. Demetrashvili

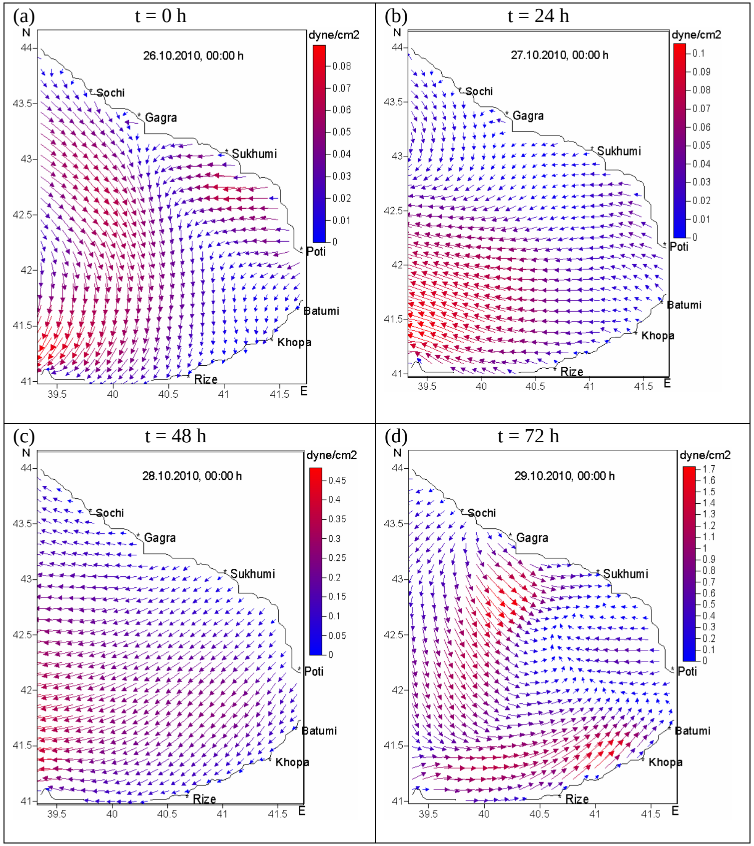

Fig. 14. Vector fields of the wind stress on the sea surface within the forecasting period: 26 October 2010, 00:00 h – 29 October 2010, 00:00 h at **(a)** 0 h, **(b)** 24 h, **(c)** 48 h, and **(d)** 72 h.

OSD
8, 397–433, 2011

A. A. Kordzadze and D. I. Demetrashvili

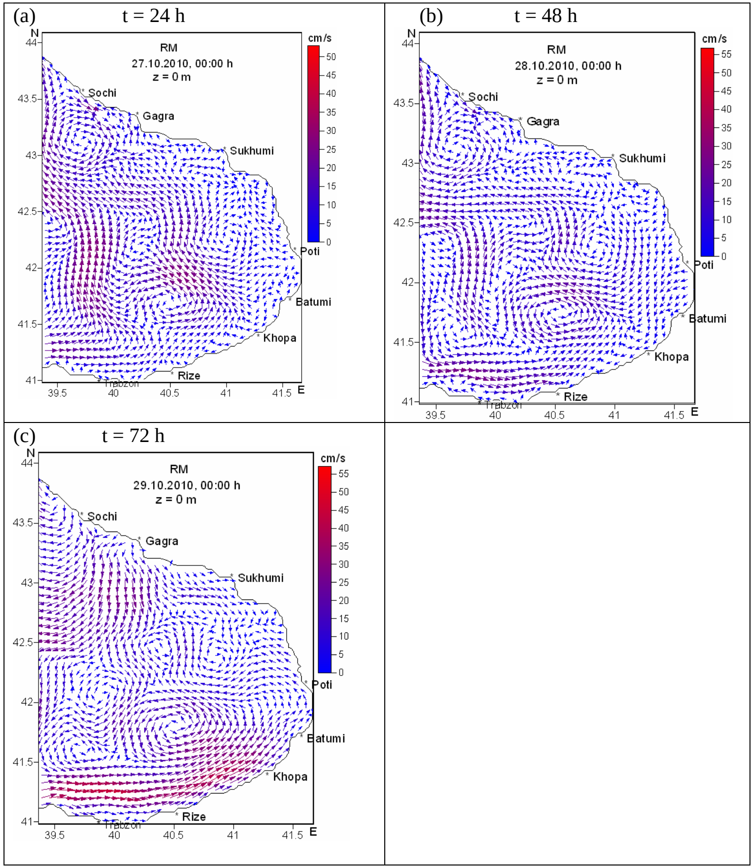

Fig. 15. The surface current fields predicted by RM-IG at **(a)** 24 h, **(b)** 48 h, and **(c)** 72 h (the forecasting period is 26 October 2010, 00:00 h – 29 October 2010, 00:00 h).

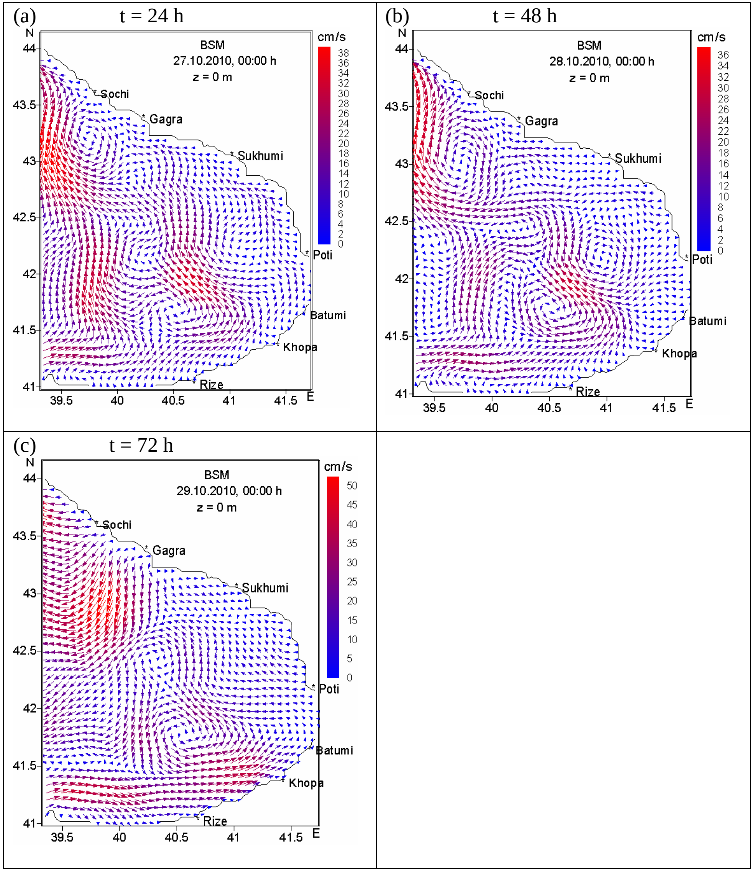

Fig. 16. The surface current fields predicted by BSM of MHI at **(a)** 24 h, **(b)** 48 h, and **(c)** 72 h (the forecasting period is 26 October 2010, 00:00 h – 29 October 2010, 00:00 h).

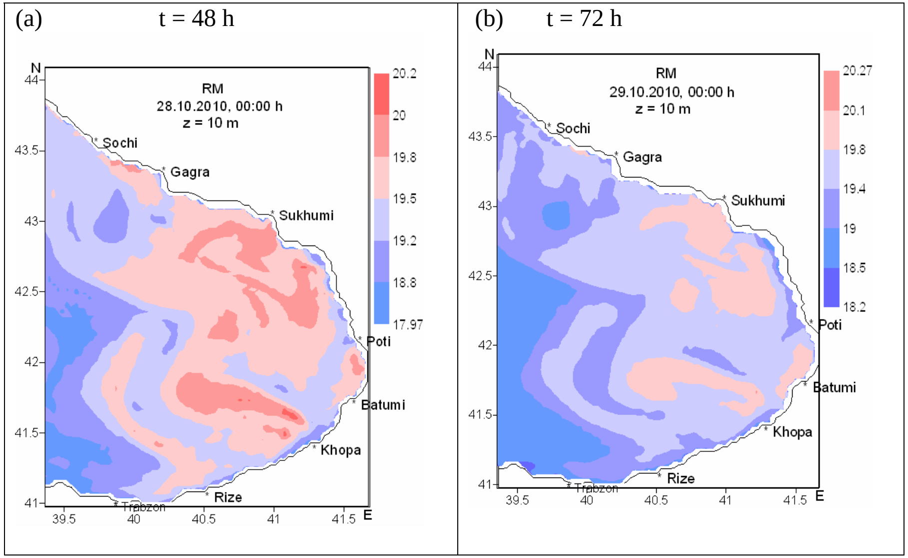

Fig. 17. The temperature fields (deg. C) on depth of 10 m predicted by RM-IG at **(a)** 48 h and **(b)** 72 h (forecasting period is 26 October 2010, 00:00 h – 29 October 2010, 00:00 h).

OSD
8, 397–433, 2011

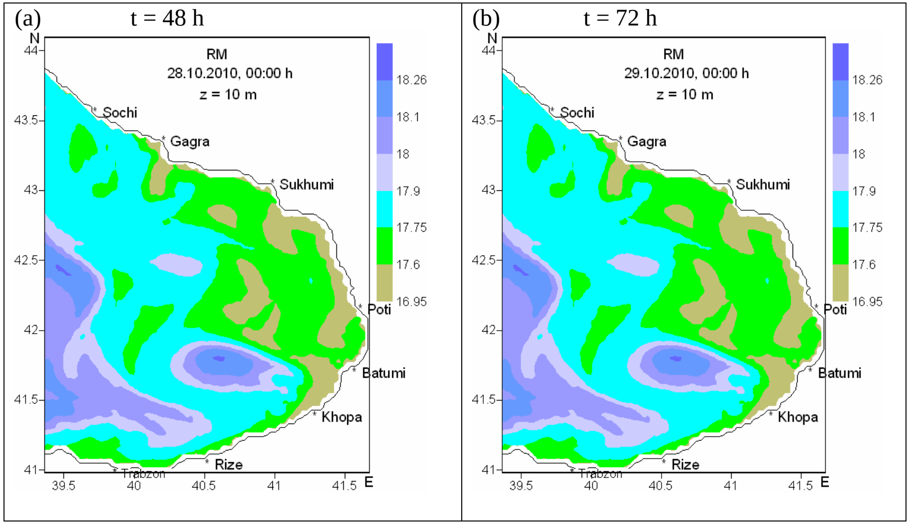

Fig. 18. The salinity fields (psu) on depth of 10 m predicted by RM-IG at **(a)** 48 h and **(b)** 72 h (forecasting period is 26 October 2010, 00:00 h – 29 October 2010, 00:00 h).

OSD
8, 397–433, 2011

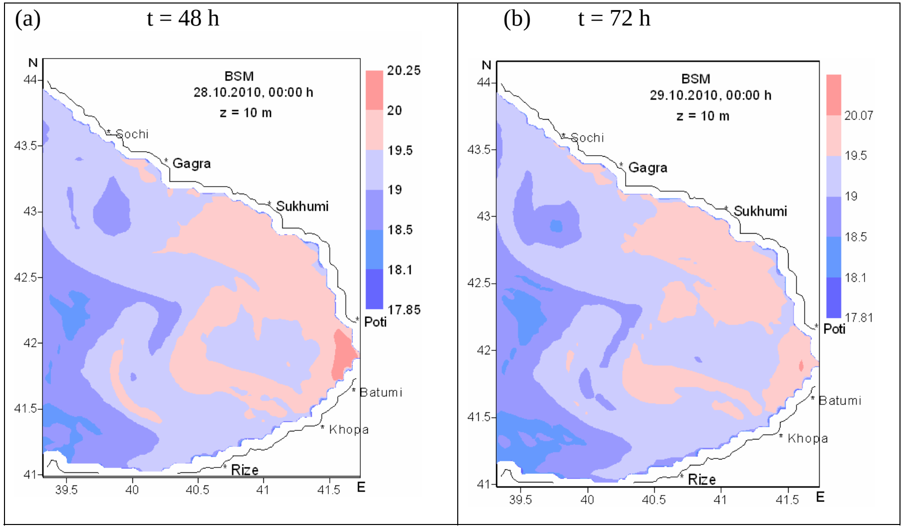

Fig. 19. The temperature fields (deg. C) on depth of 10 m predicted by BSM of MHI at **(a)** 48 h and **(b)** 72 h (forecasting period is 26 October 2010, 00:00 h – 29 October 2010, 00:00 h).

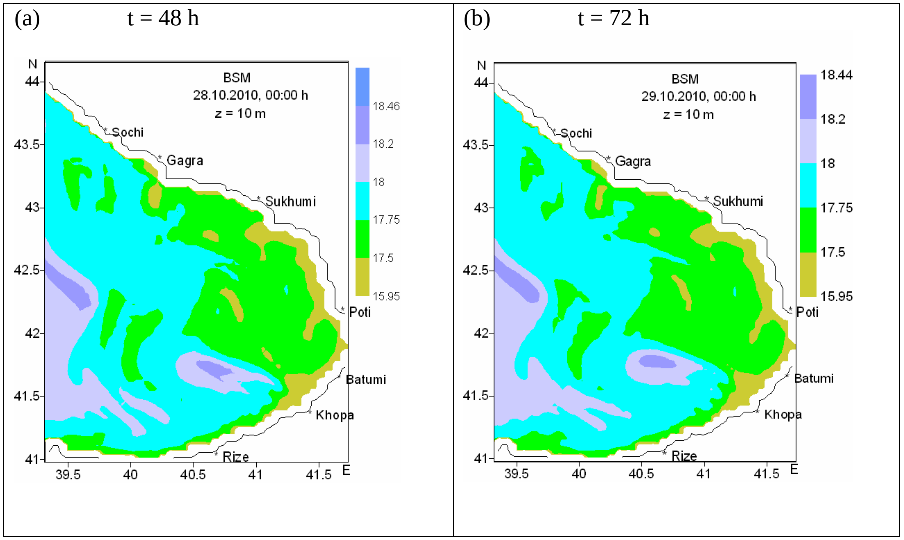

Fig. 20. The salinity fields (psu) on depth of 10 m predicted by BSM of MHI at **(a)** 48 h and **(b)** 72 h (the forecasting period is 26 October 2010, 00:00 h – 29 October 2010, 00:00 h).

OSD
8, 397–433, 2011